Figure S1

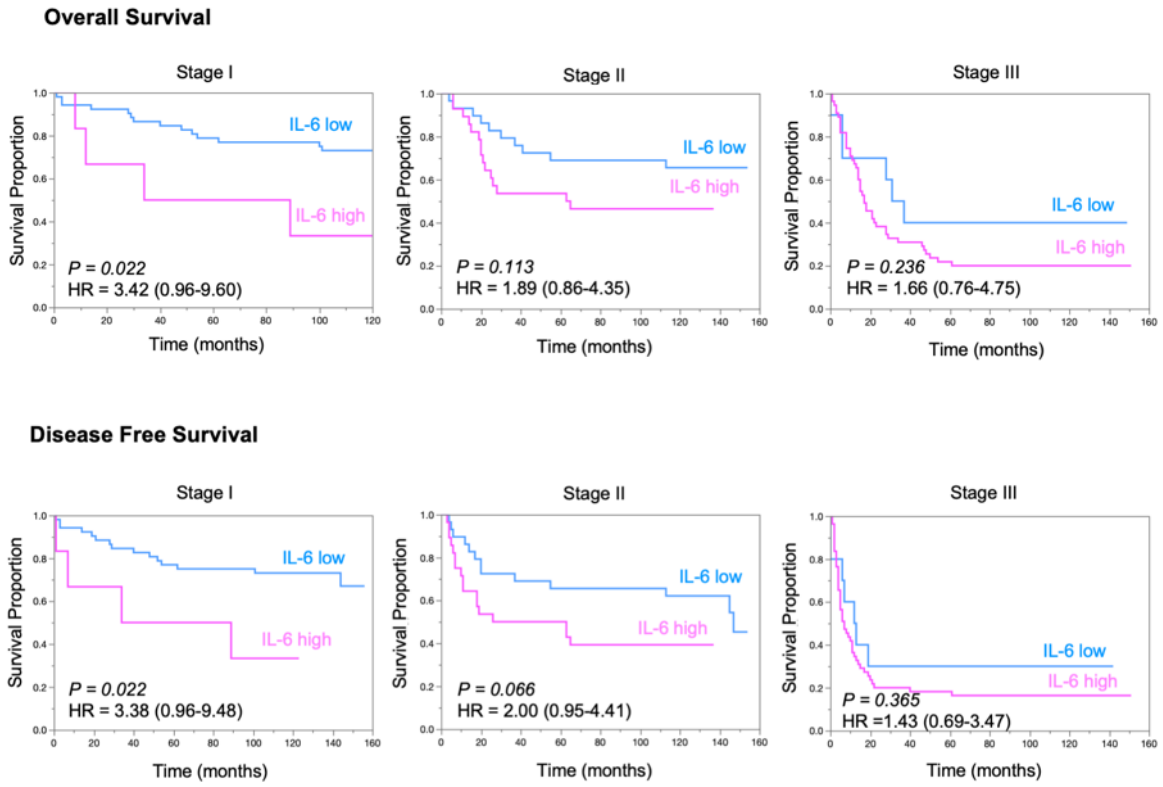

Figure S1. Subgroup analysis of IL-6 expression according to UICC Stage.

Survival curve according to IL-6 expression (low or high group). The low IL-6 group showed a significantly better prognosis at all stages (Cox regression hazard model, 95% confidence intervals, and log-rank test).

Figure S2

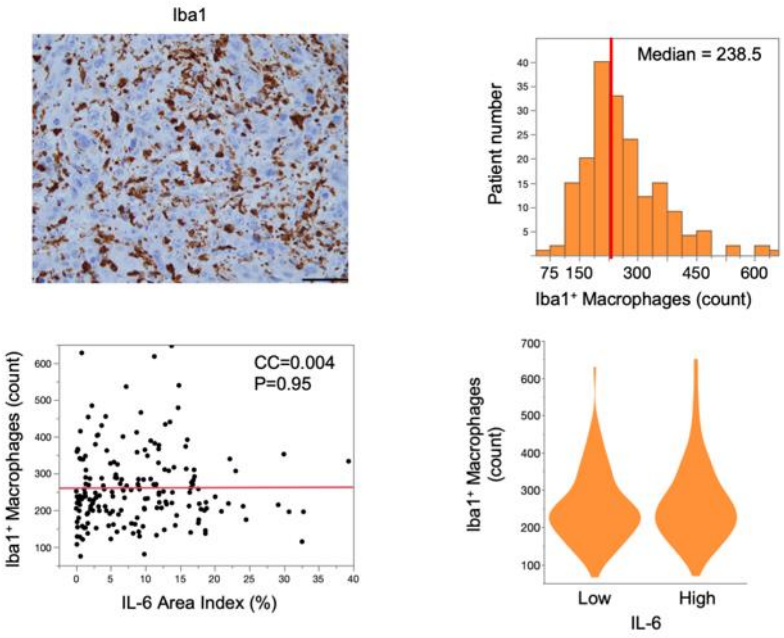

Figure S2. Correlation of IL-6 expression and TAMs distribution in esophageal cancer tissues.

The average number of Iba1$^+$ TAMs at high magnification (400×) was recorded using ImageJ. Scale bars: 50 μm (400×). The correlation between IL-6 and Iba1$^+$ TAMs is shown by scatter plot. The violin plots show comparisons based on high or low IL-6 area index.

Figure S3

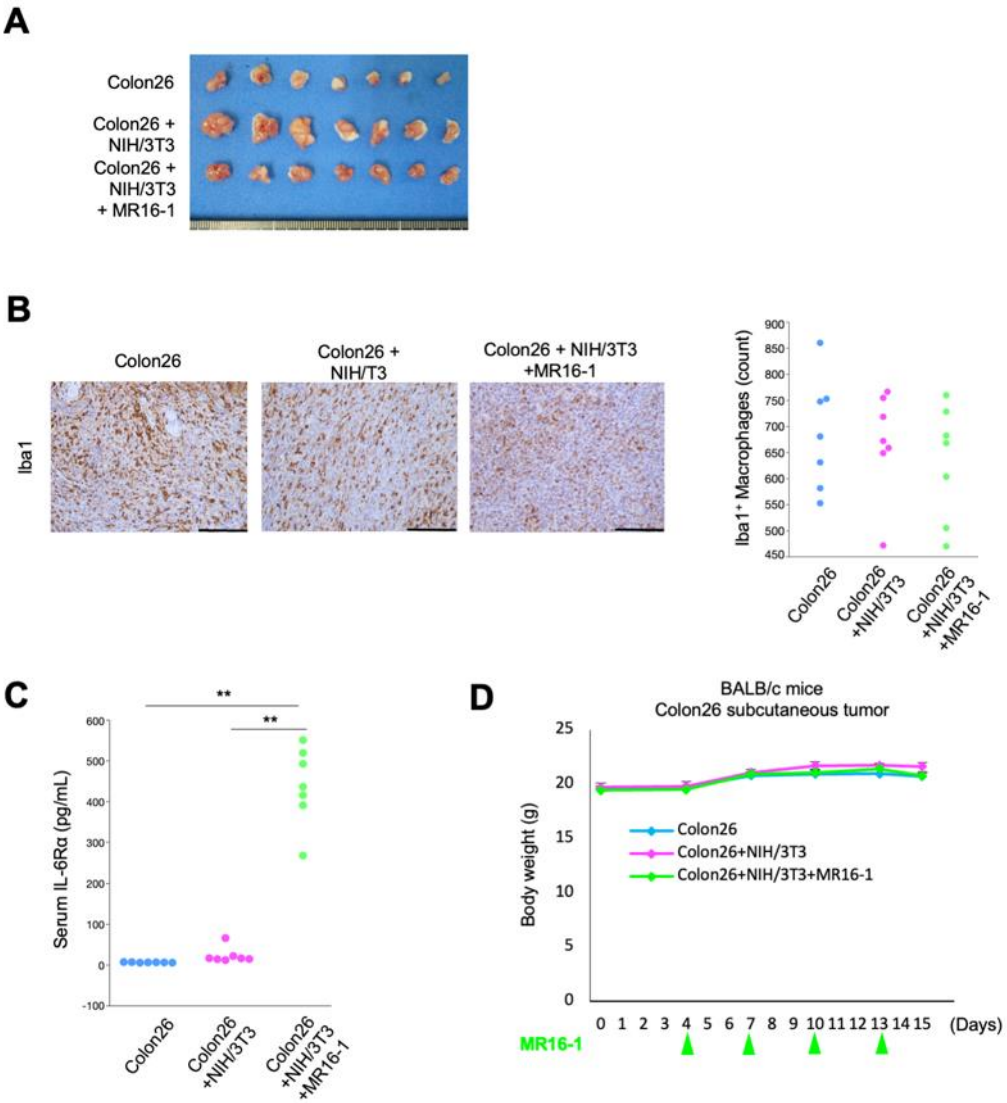

Figure S3. MR16-1 treatment for Colon26 + NIH/3T3 subcutaneous tumors in BALB/c mice.

(A) Macroscopic findings of harvested tumors; n = 7 mice/group. (B) Representative figures of immunohistochemical staining for Iba1 in tumor tissues. The average number of $Iba1^+$ TAMs at 400× magnification was recorded using ImageJ. Scale bars: 50 μm. (C) Quantification of serum IL-6Rα concentration by ELISA. $^{**}P < 0.01$, Tukey's test with ANOVA. (D) The mean body weights for each group.

Figure S4

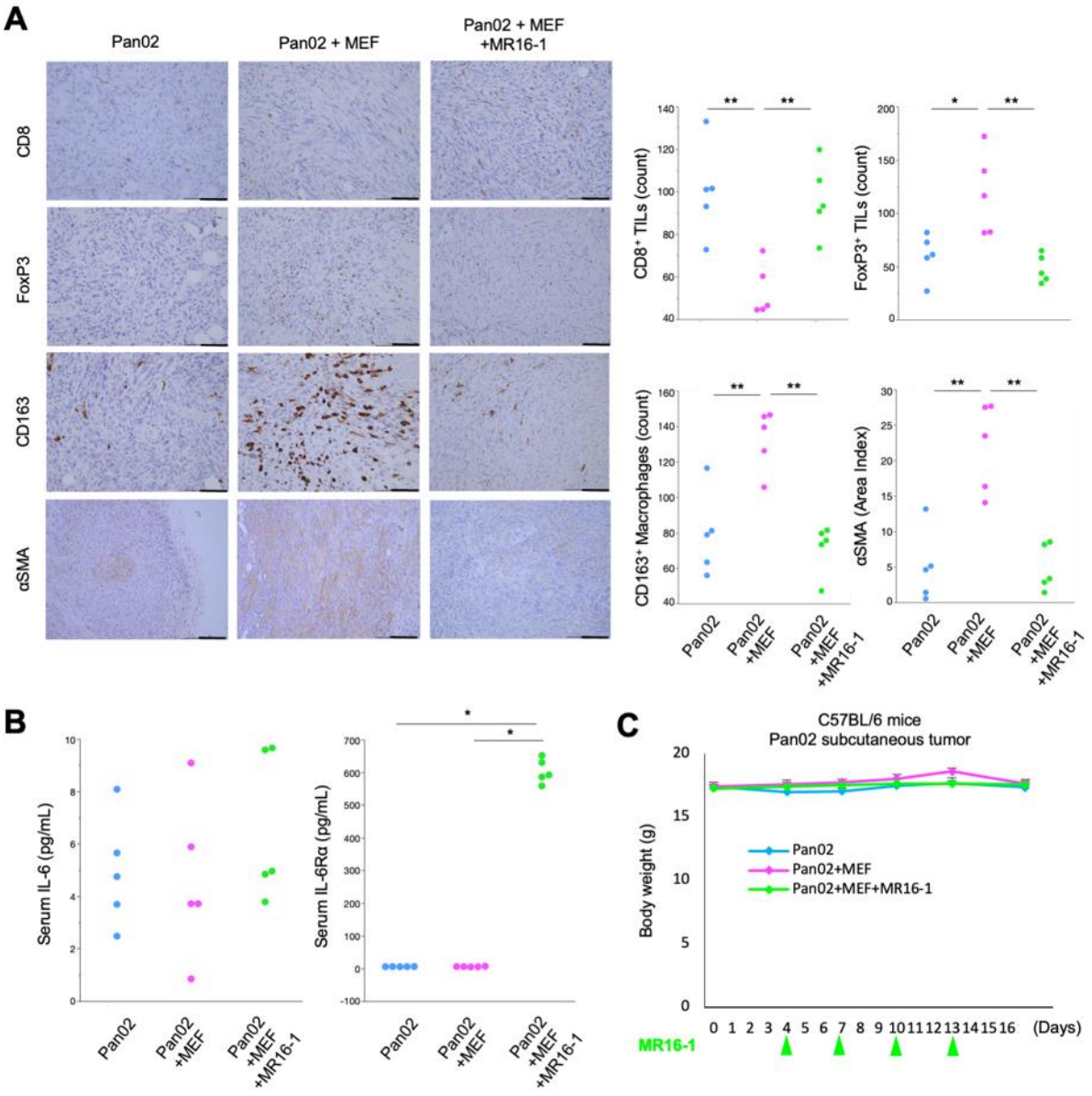

Figure S4. MR16-1 treatment for Pan02 + MEF subcutaneous tumors in C57BL/6 mice. (A) Representative figures of immunohistochemical staining for CD8, FoxP3, CD163, and αSMA in tumor tissues. The average number of $CD8^+$ or $FoxP3^+$ TILs and $CD163^+$ TAMs at 400× magnification and the area index of αSMA at 200× magnification were recorded using ImageJ. Scale bars: 100 μm (200×), 50 μm (400×). $^*P < 0.05$; $^{**}P < 0.01$, Tukey's test with ANOVA. (B) Quantification of serum IL-6 and IL-6Rα concentration by ELISA. $^*P < 0.05$. (C) Mean body weights for each group.

Figure S5

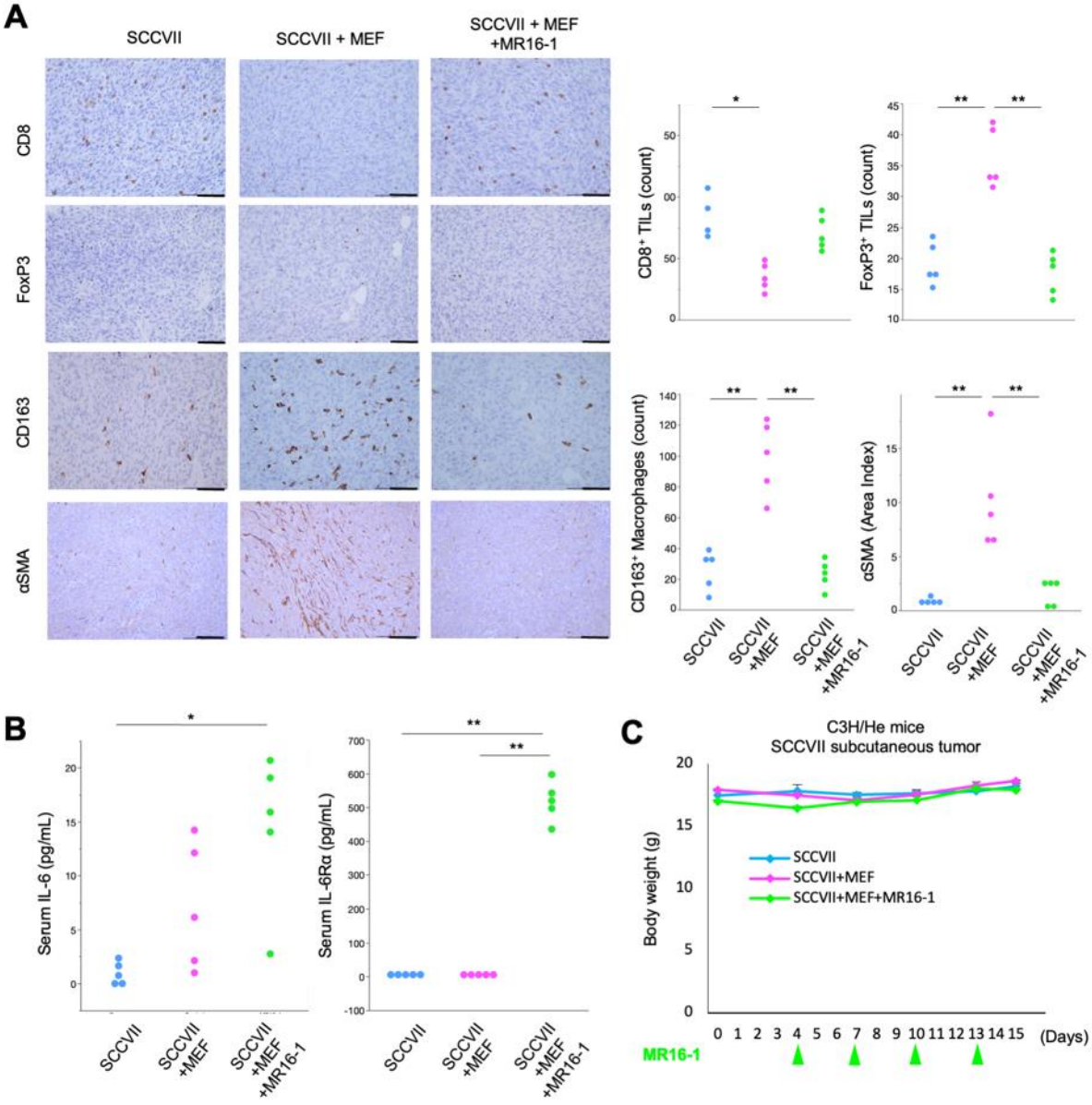

Figure S5. MR16-1 treatment for SCCVII + MEF subcutaneous tumors in C3H/He mice. (A) Representative immunohistochemical staining images for CD8, FoxP3, CD163, and αSMA in tumor tissues. The average number of $CD8^+$ or $FoxP3^+$ TILs and $CD163^+$ TAMs at 400× magnification and the area index of αSMA at 200× magnification were recorded using ImageJ. Scale bars: 100 μm (200×), 50 μm (400×). $^*P < 0.05$; $^{**}P < 0.01$, Tukey's test with ANOVA. (B) Quantification of serum IL-6 and IL-6Rα concentration by ELISA. $^*P < 0.05$, Tukey's test with ANOVA. (C) Mean body weights of each group.

Figure S6

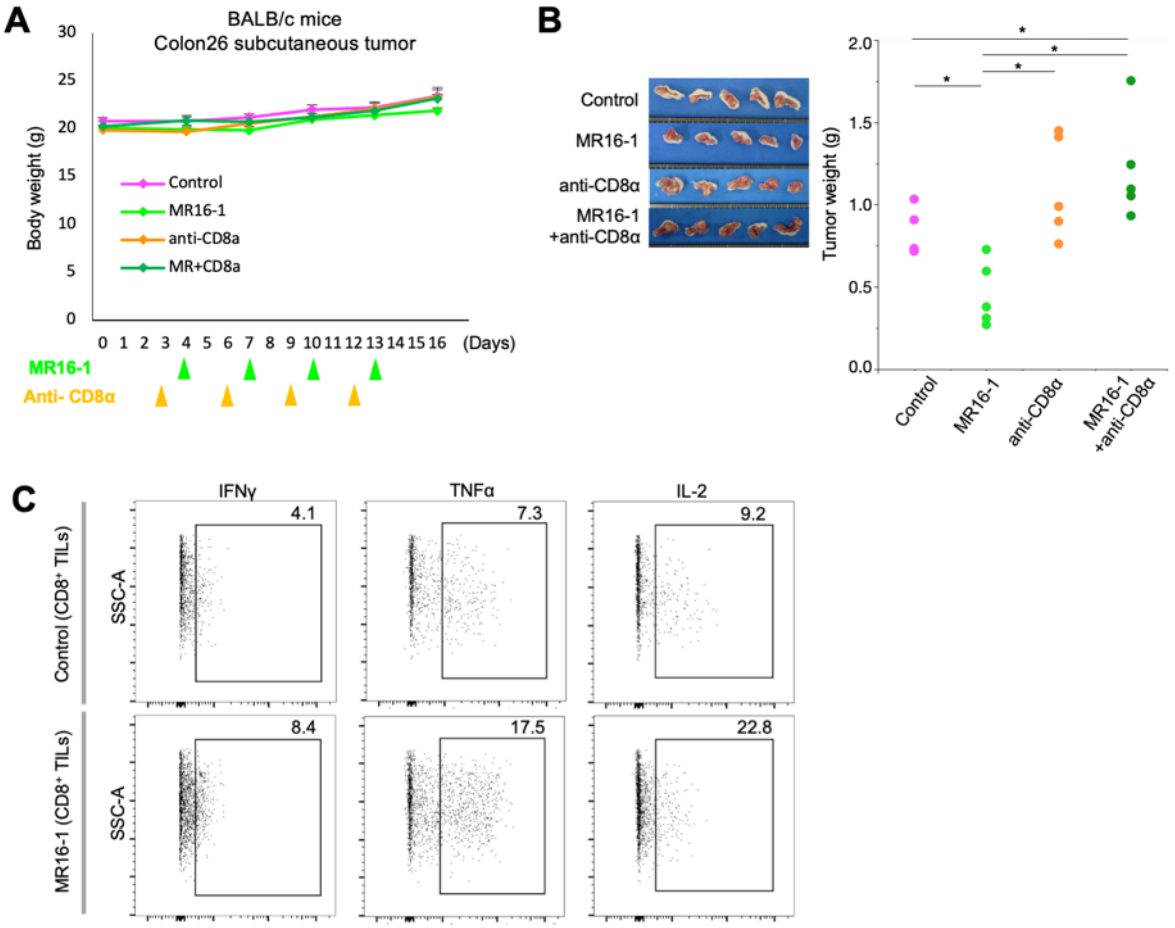

Figure S6 Treatment with MR16-1 and anti-CD8α antibody for Colon26 + NIH/3T3 subcutaneous tumors in BALB/c mice.

(A) Mean body weights for each group. (B) Macroscopic findings and weights of harvested tumors; n = 5 mice/group; mean ± SE. $^{*}P < 0.05$, Tukey's test with ANOVA. (C) Representative figures of flow-cytometric analysis: cells in the area surrounded by the black border are positive cells.

Figure S7

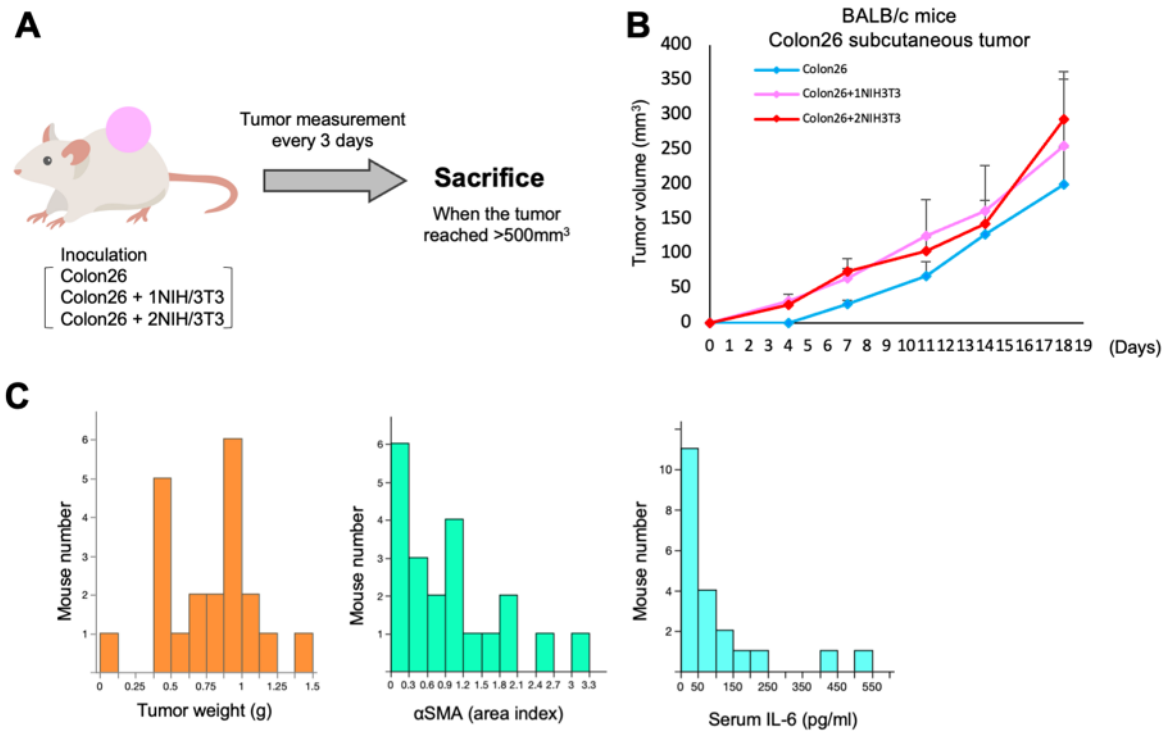

Figure S7. Protocol to assess the relationship between CAFs and serum IL-6 in Colon26 + NIH/3T3 subcutaneous tumors.

(A) Study protocol. In brief, three groups with varying amounts of co-inoculated fibroblasts of Colon26 subcutaneous tumors were harvested after the tumor volume exceeded 500 mm^3. (B) Tumor volume of the transplanted mice in each group until 18 days after inoculation. (C) Tumor weight, αSMA area index, and IL-6 area index for all mice.

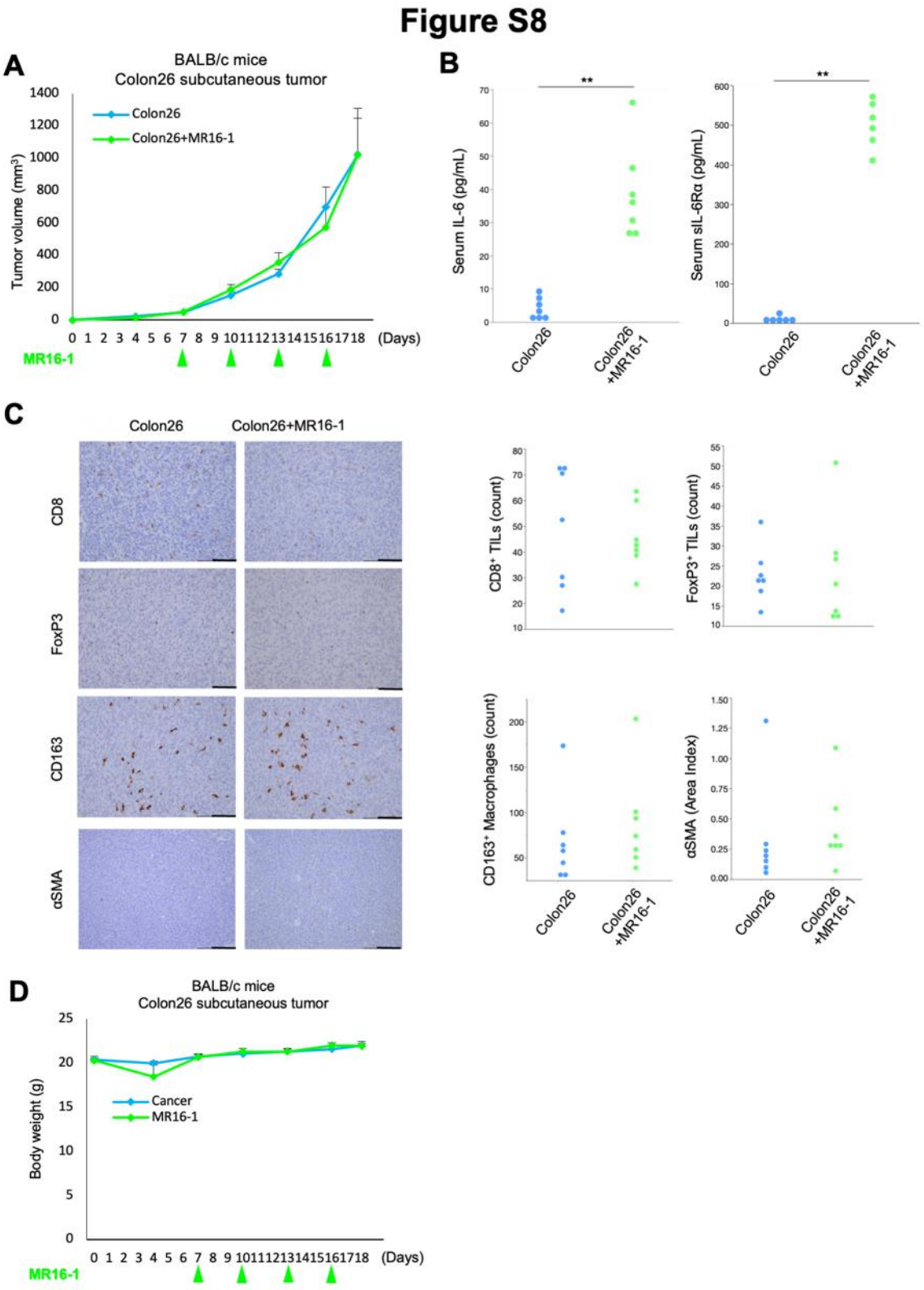

Figure S8. MR16-1 treatment for Colon26 subcutaneous tumors in BALB/c mice.

(A) Tumor volume in the transplanted mice, with or without MR16-1 treatment; n = 7 mice/group; mean ± SE. (B) Quantification of serum IL-6 and IL-6Rα concentration by

ELISA. $^{*}P < 0.05$; $^{**}P < 0.01$, Student's *t*-test. (C) Representative immunohistochemical staining for CD8, FoxP3, CD163, and αSMA in tumor tissues. Average number of $CD8^{+}$ or $FoxP3^{+}$ TILs and $CD163^{+}$ TAMs at 400× magnification and the area index of αSMA at 200× magnification were recorded using ImageJ. Scale bars: 100 μm (200×), 50 μm (400×). (D) Mean body weights of each group.

Figure S9

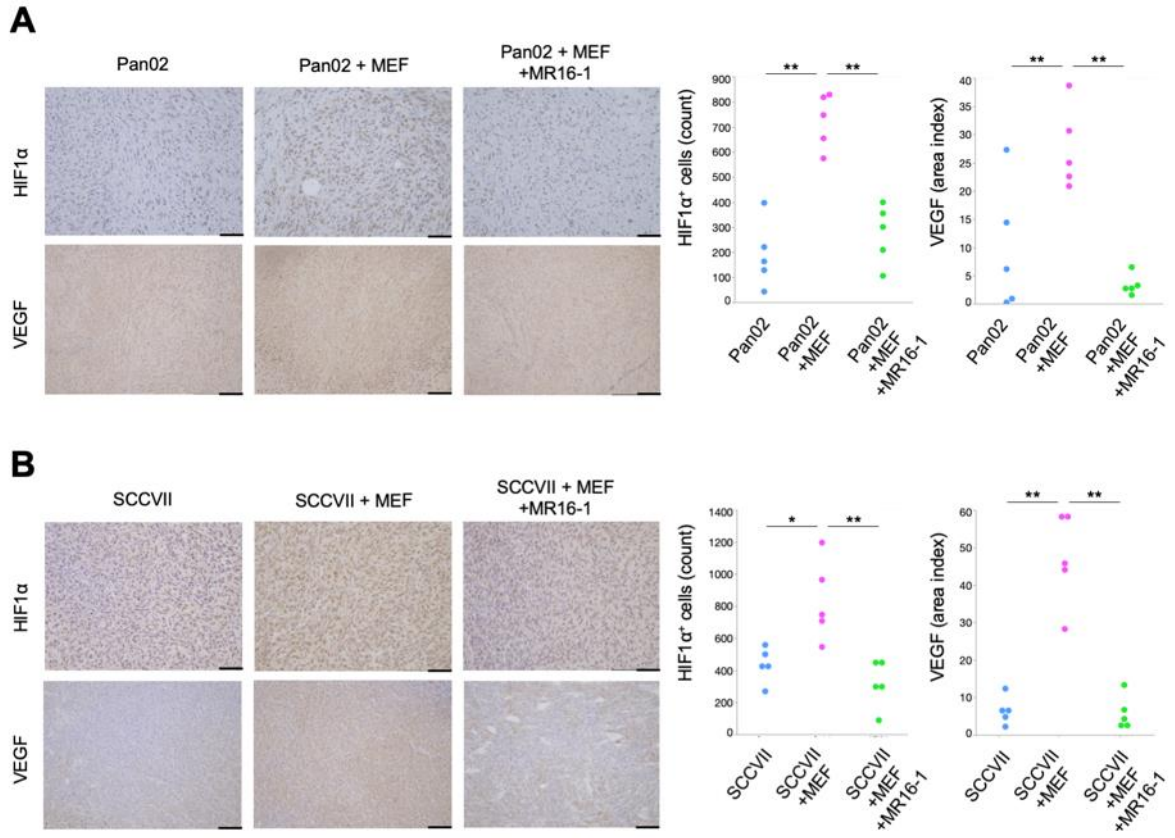

Figure S9. HIF1α and VEGF expression in Pan02 and MEF subcutaneous tumor models. (A, B) Representative immunohistochemical staining for HIF1α and VEGF in tumor tissues. Average number of HIF1α^{+} cells at 400× magnification and the area index of VEGF at 200× magnification were recorded using ImageJ software. Scale bars: 100 μm (200×), 50 μm (400×). $^{*}P < 0.05$; $^{**}P < 0.01$, Tukey's test with ANOVA. (A) Pan02 + MEF model (B) SCCVII + MEF model.

Figure S10

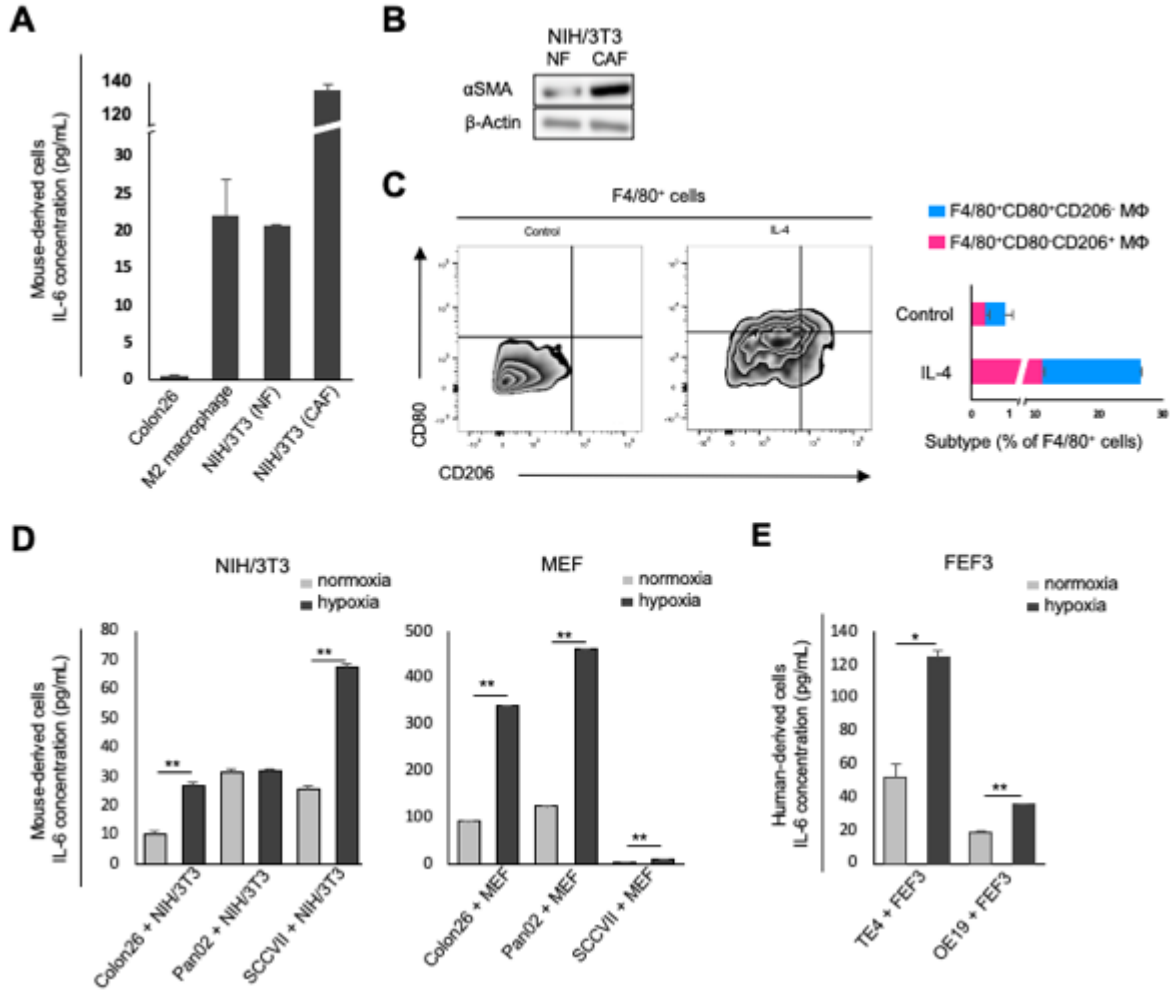

Figure S10. Cancer-associated fibroblasts are the main source of IL-6 secretion, which promote under hypoxia.

(A) Quantification of IL-6 secretion by ELISA. Cancer cells (Colon26: 0.5 × 10^6 cells), M2 macrophages (BMDM stimulated by IL-4: 0.5 × 10^6 cells), normal fibroblasts (NFs) (NIH/3T3: 0.5 × 10^6 cells), cancer-associated fibroblasts (CAFs) (NIH/3T3 stimulated by conditioned medium of Colon26: 0.5 × 10^6 cells) were seeded in 6-well plates and cultured with 10% DMEM. Culture supernatant was collected 48 h later. Data are presented as IL-6 levels per 0.1 × 10^6 cells. (B) Western blot of αSMA expression in NFs and CAFs. (C) Flow cytometry analysis of F4/80 (M1/M2 marker), and CD80 (M1 marker) on the cell surface, and intracellular CD206 (M2 marker) expression in BMDMs, with or

without IL-4 (20 ng/mL) treatment for 2 days. The bar chart shows quantification of the $F4/80^+$, $CD80^+$, and $CD206^-$ (M1) population and $F4/80^+$, $CD80^-$, and $CD206^+$ (M2) populations; n = 3. (D and E) Quantification of IL-6 secretion in co-culture model under normoxia and hypoxia. Cancer cells (0.1×10^6 cells) and fibroblasts (0.1×10^6 cells) were seeded in 6-well plates and cultured with 10% DMEM. Cells were incubated under normoxic conditions at 37 °C in a humidified atmosphere with 5% CO_2 and 20% O_2. Cells were incubated in a hypoxic chamber (Modular Incubator Chamber; Billups-Rothenberg) filled with a gas mixture of 1% O_2, 5% CO_2, and N_2. Culture supernatant was collected 48 h later. (D) Murine cell lines. (E) Human cell lines. Data are presented as IL-6 levels per 0.1×10^6 cells. $^{*}P < 0.05$; $^{**}P < 0.01$, Tukey's test with ANOVA.

Figure S11

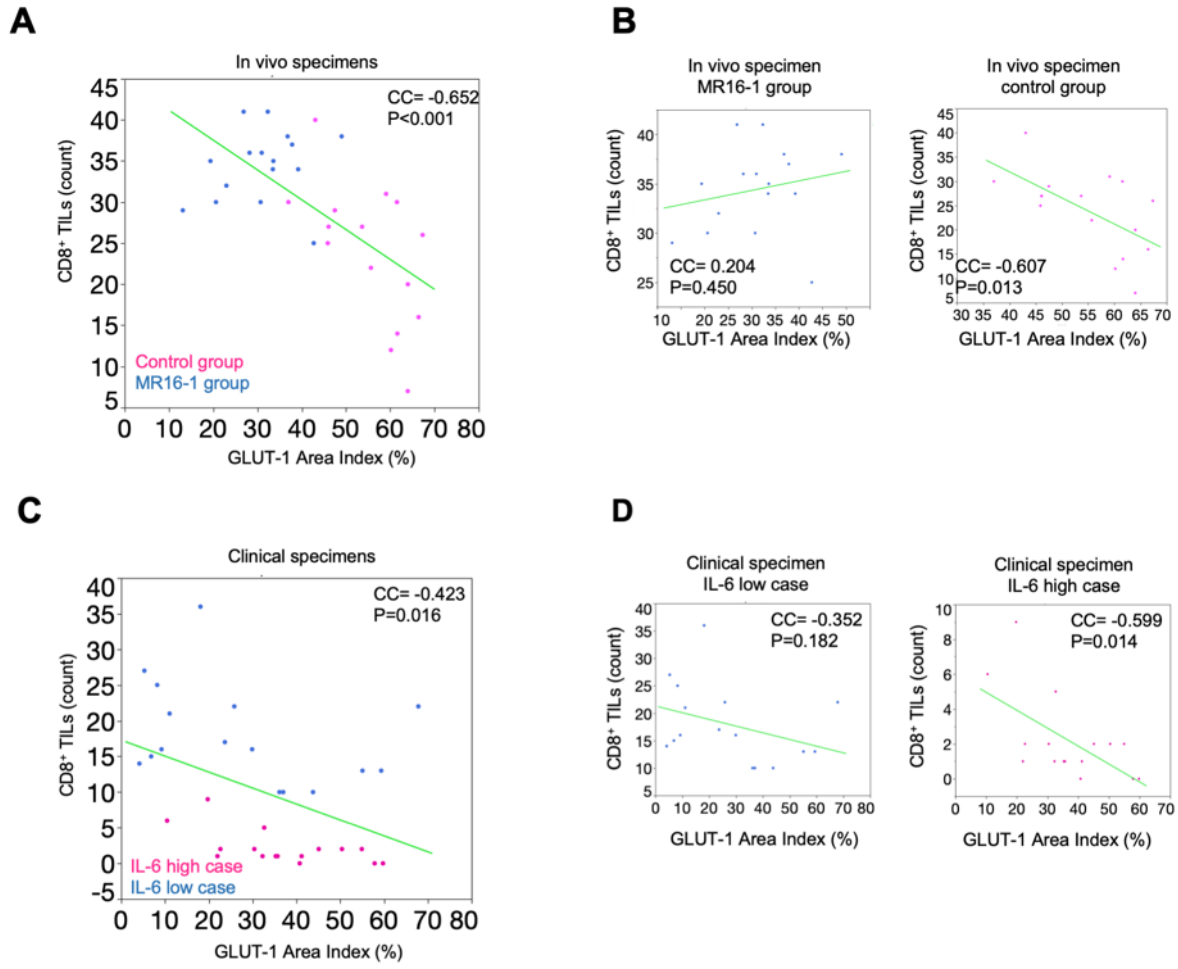

Figure S11. The relationship between GLUT-1 expression and CD8-expressing lymphocytes in the tumor microenvironment.

The number of cells expressed CD8 and GLUT-1 area index in high magnification fields of immunofluorescence images were analyzed with Image J (NIH). (B, C) The correlation between GLUT-1 and CD8-expressing lymphocytes in contol and MR16-1 treatment groups are shown by scatter plot. (D, E) The correlation between GLUT-1 and CD8-expressing lymphocytes in human esophageal cancer tissues are shown by scatter plot.

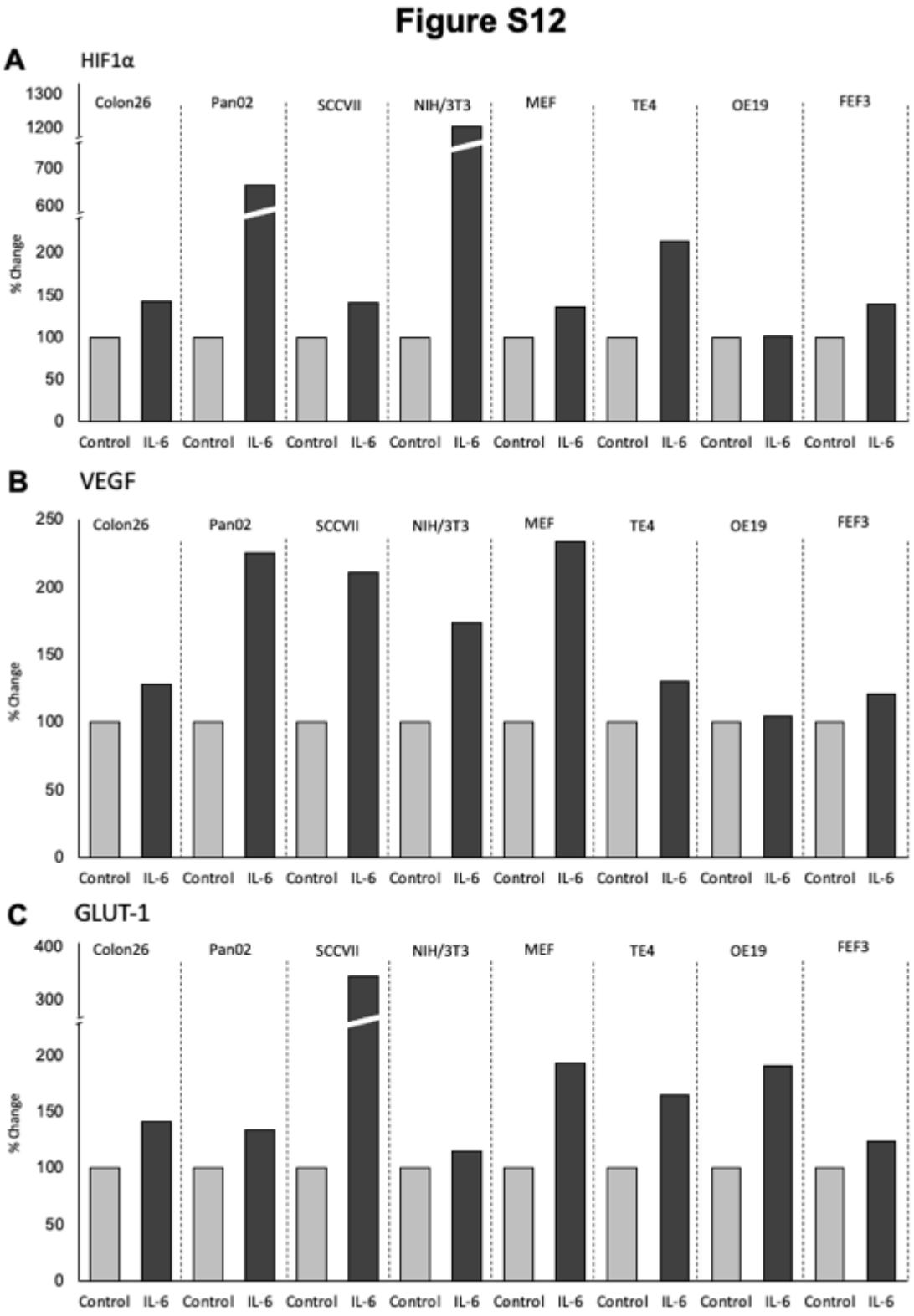

Figure S12. Densitometry of the western blot analysis.

Densitometry of the western blot analysis in Figure 6G was analyzed with Image J software (NIH). The expression was normalized to β-actin expression measured in the same sample as

an internal control. Changes are shown in percent, compared to control. (A) HIF1 α , (B) VEGF, (C) GLUT-1.

Figure S13

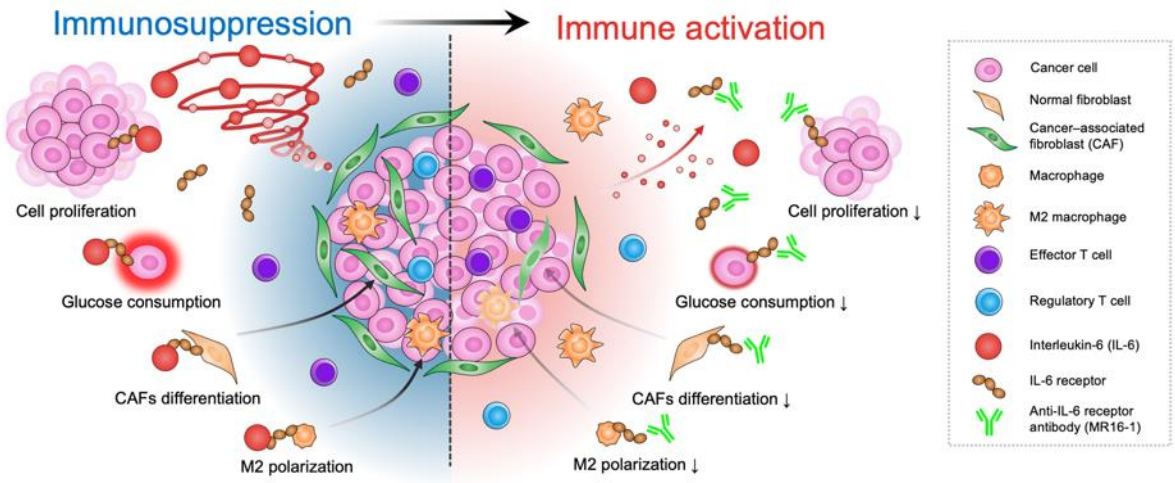

Figure S13. Schematic illustration of the effect of MR16-1 in the tumor microenvironment.

CAFs contribute to tumor progression by inducing immunosuppression via IL-6 in EC patients while MR16-1 treatment overcomes CAF-induced immunosuppression and halts tumor progress.

Table S1. List of antibodies used in this study.

Antibody	Application	Dilution	Company	Catalog no.
Anti-CD8 antibody	IHC (clinical specimens)	1:100	Dako	M7103
Anti-FOXP3 antibody [236A/E7]	IHC (clinical specimens)	1:100	Abcam	ab20034
Anti-Actin, α-Smooth Muscle antibody	IHC (clinical specimens, vivo specimens)	1:1000	Sigma-Aldrich	A5228
Anti-alpha smooth muscle Actin antibody [1A4] (FITC)	IF (clinical specimens, vivo specimens)	1:100	Abcam	ab8211
Anti-IL-6 antibody	IHC (clinical specimens)	1:4000	Abcam	ab9324
Anti-Iba1 antibody [EPR16588]	IHC (clinical specimens, vivo specimens)	1:2000	Abcam	ab178846
Anti-CD163 antibody [EPR19518]	IHC (clinical specimens, vivo specimens)	1:500	Abcam	ab182422
Purified Mouse Anti-Human HIF-1α	IHC (clinical specimens)	1:50	BD Biosciences	610959
Anti-VEGFA antibody [EP1176Y] - C-terminal	IHC (clinical specimens)	1:100	Abcam	ab52917
CD8a Monoclonal Antibody (4SM15)	IHC (vivo specimens)	1:100	eBioscience	14-0808-82
FOXP3 Monoclonal Antibody (FJK-16s)	IHC (vivo specimens)	1:100	eBioscience	14-5773-82
HIF1α	IHC (vivo specimens)	1:1000	Novus	NB100-296
VEGF	IHC (vivo specimens)	1:1000	Abcam	ab232858
Alexa Fluor® 488 F(ab')2 fragment of goat anti-mouse IgG (H+L)	IF (clinical specimens) secondary antibody	1:500	Thermo Fisher Scientific	A11017
Alexa Fluor® 568 F(ab')2 fragment of goat anti-mouse IgG (H+L)	IF (clinical specimens) secondary antibody	1:500	Thermo Fisher Scientific	A11019
Alexa Fluor® 647 F(ab')2 fragment of goat anti-mouse IgG (H+L)	IF (clinical specimens) secondary antibody	1:500	Thermo Fisher Scientific	A21237
Alexa Fluor® 647 F(ab')2 fragment of goat anti-rabbit IgG (H+L)	IF (clinical specimens) secondary antibody	1:500	Thermo Fisher Scientific	A21245
Goat anti-Rat IgG (H+L) Cross-Adsorbed Secondary Antibody, Alexa Fluor 488	IF (*vivo* specimens) secondary antibody	1:500	Thermo Fisher Scientific	A11006
Goat anti-Rat IgG (H+L) Cross-Adsorbed Secondary Antibody, Alexa Fluor 647	IF (*vivo* specimens) secondary antibody	1:500	Thermo Fisher Scientific	A21247
α-Smooth Muscle Actin (D4K9N) XP® Rabbit mAb	Western blotting	1:1000	Cell Signaling Technology	19245
HIF-1α (D2U3T) Rabbit mAb	Western blotting	1:1000	Cell Signaling Technology	14179
Anti VEGF antibody	Western blotting	1:1000	Proteintech	19003-1-AP
Anti-Glucose Transporter GLUT1 antibody [EPR3915]	Western blotting	1:1000	Abcam	ab115730
βactin	Western blotting	1:1000	Sigma-Aldrich	A5441
Zombie Aqua™ Fixable Viability Kit	FACS	1:100	BioLegend	423102
FITC anti-mouse CD8a Antibody	FACS	1:100	BioLegend	100706
Brilliant Violet 421™ anti-mouse TNF-α Antibody	FACS	1:100	BioLegend	506327
APC anti-mouse IL-2 Antibody	FACS	1:100	BioLegend	503809
APC/Cyanine7 anti-mouse IFN-γ Antibody	FACS	1:100	BioLegend	505849
Alexa Fluor® 647 anti-mouse CD80 Antibody	FACS	1:100	BioLegend	104718
PE/Cyanine7 anti-mouse F4/80 Antibody	FACS	1:100	BioLegend	123114
PE anti-mouse CD206 (MMR) Antibody	FACS	1:100	BioLegend	141706
Isotype control for Rat IgG1	*in vivo* experiment		BioxCell	BE0088
InVivoMab anti-mouse CD8α	*in vivo* experiment		BioxCell	BE0061

Table S2. Clinicopathological characteristics of esophageal cancer patients, according to Interleukin-6 (IL-6) status

Variables	Total	IL-6		*P* value
		Low (n = 92)	High (n = 93)	
Age (years)				0.575§
Median (IQR)	66 (61–72)	66 (61–72)	66 (61–71)	
Sex				0.073†
Male	163 (87.6%)	77 (83.7%)	86 (92.5%)	
Female	22 (12.3%)	15 (16.3%)	7 (7.5%)	
Histological type				0.795†
SCC	169 (27.3%)	85 (92.4%)	84 (90.3%)	
Adenocarcinoma	16 (72.7%)	7 (7.6%)	9 (9.7%)	
Neoadjuvant therapy				< 0.001†*
None	141 (41.3%)	81 88.0%)	60 (64.5%)	
Chemotherapy	31 (13.2%)	6 (6.5%)	25 (26.9%)	
Chemoradiotherapy	13 (35.5%)	5 (5.4%)	8 (8.6%)	
Pathological T stage				< 0.001†*
T1	77 (41.3%)	68 (73.9%)	9 (9.7%)	
T2	23 (13.2%)	10 (10.9%)	13 (14.0%)	
T3	79 (35.5%)	13 (14.1%)	66 (71.0%)	
T4	6 (9.9%)	1 (1.1%)	5 (5.4%)	
Pathological N stage				< 0.001†*
N0	84 (53.7%)	62 (67.4%)	22 (23.7%)	
N1	42 (19.0%)	16 (17.4%)	26 (28.0%)	
N2	38 (14.0%)	7 (7.6%)	31 (33.3%)	
N3	21 (13.2%)	7 (7.6%)	14 (15.1%)	
Pathological stage				< 0.001†*
I	58 (10.7%)	52 (56.5%)	6 (6.5%)	
II	57 (24.8%)	29 (31.5%)	28 (30.1%)	
III	65 (2.5%)	10 (10.9%)	55 (59.1%)	
IV	5 (4.1%)	1 (1.1%)	4 (4.3%)	
αSMA				< 0.001§*
Median (IQR)	8.99 (4.03–16.17)	4.03 (2.50–6.86)	15.75 (10.89–20.48)	

(continued)

Tumor-infiltrating lymphocytes				
CD8+				< 0.001§*
Median (IQR)	32.75 (17.50–57.00)	42.63 (26.00–69.69)	21.50 (11.88–46.50)	
FoxP3+				< 0.001§*
Median (IQR)	16.33 (8.00–28.50)	9.63 (3.81–16.25)	24.25 (16.54–36.00)	
Tumor-associated macrophages				
Iba1+				0.335§
Median (IQR)	238.50 (197.88–310.13)	237.25 '193.69–294.63)	248.50 (201.25–314.38)	
CD163+				< 0.001§*
Median (IQR)	208.50 (116.00–284.38)	116 (74.31–218.06)	252.75 (206.75–321.75)	

Student's *t*-test: §, Fisher's exact test: †, Statistical significance: $P < 0.05$, IQR: interquartile range, SCC: squamous cell carcinoma

Table S3. Results of univariate and multivariate Cox regression analyses of factors associated with disease-free survival among esophageal cancer patients.

		Univariate analysis			Multivariate analysis		
Variable	**Unfavorable/Favorable**	**HR**	**95%CI**	***P* value**	**HR**	**95%CI**	***P* value**
Histological type	Adenocarcinoma/SCC	0.62	0.29–1.34	0.227			
Pathological T stage	T3-4/T1-2	4.09	2.73–6.13	< 0.001*	2.61	1.57–4.33	< 0.001*
Pathological N stage	N1-3/N0	2.51	1.67–3.76	< 0.001*			
Neoadjuvant therapy	yes/no	2.66	1.76–4.03	0.001*	1.88	1.22–2.88	0.004*
αSMA	high/low	2.64	1.77–3.93	< 0.001*			
IL-6	high/low	3.29	2.19–4.96	< 0.001*	1.76	1.06–2.92	0.028*
Tumor-infiltrating lymphocytes							
CD8+	high/low	0.62	0.42–0.91	0.014*			
FoxP3+	high/low	2.46	1.65–3.67	< 0.001*			
Tumor-associated macrophages							
Iba1+	high/low	1.23	0.84–1.80	0.286			
CD163+	high/low	1.66	1.13–2.43	0.010*			

Cox proportional hazard model, Statistical significance: $P < 0.05$, HR: hazard ratio, CI: confidence interval, SCC: squamous cell carcinoma, SMA: smooth muscle actin, IL-6: interleukin-6, FoxP3: forkhead box p3, Iba1: ionized calcium-binding adaptor protein1